An analysis of the multiscale nature of tropical cyclone activities in June 2004: Climate background

Lin Ching,[1] Chung-Hsiung Sui,[1,2] and Ming-Jen Yang[1,2]

[1] A record-breaking five tropical cyclones (TCs) formed in June 2004 in the western North Pacific (WNP), where June is normally a transition month to the typhoon season and therefore sensitive to climate oscillations. This special month (June 2004) was an unusual period in the developing stage of a warm (El Niño) episode and a strong convective phase of the Madden-Julian Oscillation (MJO). Such climate background is shown to provide large-scale favorable circulations for TC formation: the warm sea surface temperature anomalies (SSTAs) associated with developing El Niño and convective heating of the MJO to jointly induce weaker easterly trade winds and a large-scale cyclonic circulation anomaly in the WNP. A space-time filtering of the outgoing longwave radiation (OLR) and 850 hPa wind fields is performed to identify the MJO, Rossby waves, and mixed Rossby-gravity (MRG) waves (or tropical depression (TD)-type disturbances). From the evolution and structure of these high-frequency waves in relation to that of the MJO and the climate background, the heating and enhanced low-level cyclonic flow in the WNP associated with the MJO and climate background are attributed to the initiation, propagation, and energy dispersion of tropical Rossby and MRG-TD waves, interacting with convection. The relative importance of these large-scale waves to the five TC formations (A–E) is quantified by examining the normalized vorticity at 850 hPa and OLR at the genesis location of each TC. TCs A and C (TCs B and D) were related to the Rossby wave (the MJO), and the MRG-TD was the most related to TC E.

1. Introduction

[2] The 25-year-averaged number of tropical cyclone (TC) formations (from 1982 to 2006) in the western North Pacific (WNP) is 31.28 based on the best track data archived by the Joint Typhoon Warning Center (JTWC). The annual number of TC formations in 2004 was 32. While this is similar to the climatological value, more TCs formed in June and August 2004, and 10 typhoons made landfall over Japan in 2004, which was 4 times larger than the climatology (2.6) based on Japan Meteorological Agency (JMA). A few studies have investigated this unusual event. For example, *Kim et al.* [2005] found that the weakened North Pacific subtropical high (NPSH) in the summer of 2004 caused unusually high number of landfalling TCs in Japan. They also mentioned that the summer of 2004 was in an early stage of a warm (El Niño) episode, and the associated strong cyclonic anomalies accompanied by widely organized deep convection in the WNP provided favorable conditions for cyclogenesis. *Nakazawa* [2006] also investigated the typhoon season of 2004 and found that the monsoon trough was enhanced during the convective phase of the Madden-Julian Oscillation (MJO) [*Madden and Julian*, 1971] over the WNP and generated most of the TCs over that region in 2004.

[3] Many studies have been performed to examine the influence of the circulation associated with the warm SSTAs in the central Pacific on TC activity in the WNP [*Chan et al.*, 1998; *Chia and Ropelewski*, 2002; *Wang and Chan*, 2002; *Chen et al.*, 2004, 2006; *Camargo and Sobel*, 2005; *Hsu et al.*, 2009]. These studies found that TC activity is linked to anomalies in large-scale flow patterns at the low-tropospheric level that are related to TC genesis and development. These studies also found that the increase of the low-level shear vorticity generated by El Niño–induced equatorial westerlies influences the favorable region of TC genesis, i.e., enhances TC activity over the southeast portion of the WNP, while the upper-level convergence induced by the deepening of the east Asian trough and the strengthening of the NPSH may suppress TC genesis over the northwest portion of the WNP. For more details, see reviews offered by *Landsea* [2000], *Chu* [2004], and *Chan* [2005].

[1]Department of Atmospheric Sciences, National Central University, Taipei, Taiwan.
[2]Institute of Hydrological and Oceanic Science, National Central University, Taipei, Taiwan.

[4] The relationship between TC activity and the MJO has been extensively studied [e.g., *Nakazawa*, 1986; *Liebmann et al.*, 1994; *Molinari et al.*, 1997; *Molinari and Vollaro*, 2000; *Maloney and Hartmann*, 2000a, 2000b, 2001; *Hall et al.*, 2001; *Straub and Kiladis*, 2003; *Bessafi and Wheeler*, 2006; *Frank and Roundy*, 2006; *Harr*, 2006; *Ho et al.*, 2006; *Kim et al.*, 2008]. These studies indicate a regional contrast in the TC-MJO relation; that is, the relation is much more evident in the eastern Pacific compared to the western Pacific. *Liebmann et al.* [1994] examined the relationships between the MJO and TCs in the western Pacific and Indian oceans. They found that cyclones preferentially occur in the MJO convective phase at the region and also noted that the interaction between the TC activity and wave variations on different scales is important. *Kim et al.* [2008] examined the relationship between the TC activity in the WNP and the phase of the MJO during the summer (June to September) from 1979 to 2004. The number of TC genesis increases when the MJO-related convective region moved into the WNP and the genesis region follows the propagation of the MJO-related convective region.

[5] The theory of equatorially trapped waves has been studied extensively since the pioneering works by *Matsuno* [1966], *Yanai and Maruyama* [1966], and *Lindzen* [1967]. Tropical convection can be diagnosed into the zonal propagation of convective disturbances based on the linear equatorial wave modes [*Takayabu*, 1994; *Wheeler and Kiladis*, 1999; *Wheeler et al.*, 2000]. *Wheeler and Kiladis* [1999] performed a wave number-frequency spectral analysis to identify the zonally propagating waves in deep tropical convection, which corresponds well to the dispersion relations of the equatorially trapped wave modes. This method is helpful to recognize the variations of the zonal propagating waves.

[6] MJO is usually identified as an eastward-propagating intraseasonal oscillation (ISO). Some studies note that the ISO also provides the favorable condition for the development of a tropical depression (TD)-type disturbance. The structure of the TD-type disturbance has been well described [*Lau and Lau*, 1990, 1992; *Chang et al.*, 1996]. The westward-propagating mixed Rossby-gravity (MRG) wave and the TD-type disturbance (hereafter MRG-TD) are more active in the strong ISO convective phase (i.e., low-level westerly phase) [*Maloney and Dickinson*, 2003; *Straub and Kiladis*, 2003]. *Straub and Kiladis* [2003] pointed out that the westward-propagating MRG-TD wave is enhanced within the low-frequency ISO convective envelope, allowing the MRG-TD convection to project onto the low-frequency ISO signal. The ISO and high-frequency variations such as quasi-biweekly oscillations and TCs may not be independent, which means that they are a multiscale interactive system. This is particularly evident in the western Pacific warm pool region [*Ko and Hsu*, 2006, 2009; *Hsu et al.*, 2008; *Chen and Huang*, 2009; *Chen and Sui*, 2010].

[7] TC formation is frequent in July, August, and September. June is in a transition month to the typhoon season, so that the large-scale conditions in June are not as favorable as those during the typhoon season. In such a period, TC genesis may be more sensitive to any favorable large-scale condition. During the warm season of 2004, the MJO amplitude was significantly large and the MJO accompanied many high-frequency waves. Those high-frequency wave variations also contributed to TC genesis. Five TCs formed in June 2004. This record-breaking event of TC genesis is a good case to investigate how the multiscale waves interact with TC activity. It should be examined from the climate background and the interaction of multiscale wave activity.

[8] This paper is organized into five sections. Section 2 describes the data and methods used. Section 3 discusses the correlation between TC genesis and the El Niño-Southern Oscillation (ENSO). Section 4 discusses the relationship between TC genesis and the MJO. We analyzed the tropical waves and their relation with the MJO and TCs in section 5. Finally, a summary and discussion are presented in section 6.

2. Data and Methods

[9] This study used the 6-hourly horizontal wind field and the relative vorticity at 850 hPa obtained from the National Centers for the Environmental Prediction (NCEP) reanalysis version 2 (R2) [*Kanamitsu et al.*, 2002] to examine large-scale circulation characteristics, because the data length (from 1979 to the present) is longer than the satellite-based data, so that it is suitable for climatic statistical analysis. The R2 data set is provided on a 2.5° × 2.5° latitude-longitude grid. In addition to the R2 data, we also used another global assimilation data set produced by the NCEP Global Data Assimilation System (GDAS) that has been archived at National Climatic Data Center back to 1997 [*Kanamitsu*, 1989]. The NCEP GDAS is the final run in the series of NCEP operational runs. NCEP postprocessing of GDAS converts the data from the spectral coefficient at sigma levels to 1° latitude-longitude grid at mandatory pressure levels. These final (FNL) gridded analysis data are utilized to analyze the detailed structure of waves and TCs. The 6-hourly FNL data are available for the period from 30 July 1999 to the present. In addition, the daily optimum interpolation SST (OISST) [*Reynolds et al.*, 2007] obtained from the National Oceanic and Atmospheric Administration (NOAA) is also used in this study for climatological analyses. The data length is from November 1981 to the present.

[10] The daily interpolated outgoing longwave radiation (OLR) [*Liebmann and Smith*, 1996] obtained from the NOAA polar orbiting satellite is used as a proxy for deep tropical convection. We perform the wave number-frequency spectral analysis as described by *Wheeler and Kiladis* [1999] to extract the MJO, equatorial Rossby wave, and MRG-TD wave. While the OLR is used to present further evidence of the MJO, the relative vorticity and meridional wind are used to present further evidence of equatorial Rossby wave and MRG-TD wave, respectively. The MJO signal is extracted by retaining only those eastward-moving spectral components that correspond to zonal wave numbers 0–5 and periods 30–90 days. The equatorial Rossby wave corresponds to westward-moving components of zonal wave numbers 1–10 and periods 10–40 days. The MRG-TD wave corresponds to westward-moving components of zonal wave numbers 0–14 and periods 2.5–10 days.

[11] TC formation in the WNP from 1982 to 2006 is based on the best track data from the JTWC [*Chu et al.*, 2002], which is a postseason reanalysis using additional information. The data contain the date, time, latitude, longitude, and intensity in every 6 h for all storms designated by the JTWC as being TD strength or greater. The JTWC best track data

Year	1982	1983	1984	1985	1986	1987	1988	1989
TC	3	1	2	2	2	2	2	2
MJO	act 27.4		act 25.1	act 31.2	act 27.4	act 21.8	inact 19.9	
	1990	1991	1992	1993	1994	1995	1996	1997
	3	1	2	1	2	2	0	3
		act 21.4				inact 25.2	inact 23.5	inact 34.6
1998	1999	2000	2001	2002	2003	2004	2005	2006
0	1	0	2	3	2	5	0	2
				act 19.9	inact 32.8	act 23.9	inact 19.6	inact 27.4

Figure 1. Numbers of western North Pacific tropical cyclones in June, 1982–2006. Light (dark) gray boxes represent ENSO warm (cold) years based on Oceanic Niño Index (ONI) in December–February (DJF). The italic and bold type represents the TC numbers of TC-active years (more than three TCs occur). Those for TC-inactive years (no TC) are denoted in bold type with underline. The average number of TC in June from 1982 to 2006 is 2. The MJO-active and -inactive events are marked "act" and "inact," respectively, along with measures of MJO strength (numbers below) based on RMM indices, i.e., the summation of amplitude of active phase (5, 6, 7) or inactive phase (1, 2, 3) in June larger than two thirds of mean MJO amplitude in June (19.58).

are available from 1945 to the present. A tropical storm is defined as a TC with the maximum wind speed larger than 34 knots, which is called "typhoon" in the WNP. The cyclogenesis time (i.e., warning time) is defined as the time of first warning based on the best track data.

[12] From the best track data, we divide the 25 months of June into TC-active (1982, 1990, 1997, 2002, 2004), TC-inactive (1996, 1998, 2000, 2005), and normal categories (remaining years). The TC-active (inactive) category refers to those months of June when there are more than 3 TCs (no TC), which is above (below) the climatological averaged number plus (minus) one standard deviation. Next, we divide the 25 months of June into the developing warm (1982, 1986, 1987, 1994, 1997, 2002, 2004, 2006), developing cold (1984, 1988, 1998, 1999, 2000), and normal events based on the Oceanic Niño Index (ONI) [Xue et al., 2003]. The warm and cold events are defined as follows. If five consecutive months are at or above the +0.5° anomaly for warm (El Niño) events and at or below the -0.5° anomaly for cold (La Niña) events. We also divide the 25 months of June into the MJO-active and -inactive periods based on the real-time multivariate MJO (RMM) indices [Wheeler and Hendon, 2004]. The MJO-active period is defined when the RMM indices are in phases 5, 6, or 7 in June (deep convection associated with the MJO affects the WNP) and the corresponding mean amplitude is larger than two thirds of the climatological mean MJO amplitude in June (19.58). The MJO-inactive period is similarly defined except for the RMM indices in June are in phases 1, 2, or 3. The large amplitude means that the MJO is strong or has a long lifetime. There are eight MJO-active Junes (1982, 1984, 1985, 1986, 1987, 1991, 2002, and 2004), and seven MJO-inactive Junes (1988, 1995, 1996, 1997, 2003, 2005, and 2006).

[13] In order to determine the relation between major tropical waves and TC formation, we define a wave-related (WR) index within the 5° × 5° box surrounding a TC center. We normalize the area-mean value of the OLR and vorticity fields of each wave on the cyclone center by the corresponding standard deviation, which is calculated by all 25 months of June.

3. Modulation by ENSO

[14] Because June is normally in the developing stage of an El Niño or La Niña episode, we examine the SST in Niño3.4 (5°S–5°N, 120°W–170°W) from May to July (MJJ) and from December to the following February (DJF) according to the ONI. The SST in MJJ and the number of TC genesis in June appears not significantly correlated (their correlation coefficient is only 0.25). Instead, the number of TC genesis in June is better correlated with the SST in DJF (correlation coefficient 0.5, significant at the 99% confidence level). To further analyze their relationship, we summarize the number of TCs over the WNP in June from 1982 to 2006 (Figure 1), and labeled the nine El Niño developing years by gray shading based on the ONI (1982, 1986, 1987, 1991, 1994, 1997, 2002, 2004, and 2006). The month of June in these El Niño years all had at least one TC and four of them had three TCs or more (TC-active). It shows a tendency that more TCs formed in June at the developing stage of an El Niño episode. Figure 1 also shows number of TCs in six La Niña episodes (1984, 1988, 1995, 1998, 1999, and 2000). Among these months of June, two were TC-inactive but three had two TCs. There is no apparent relationship between the developing stage of a La Niña episode and the number of TC genesis in June.
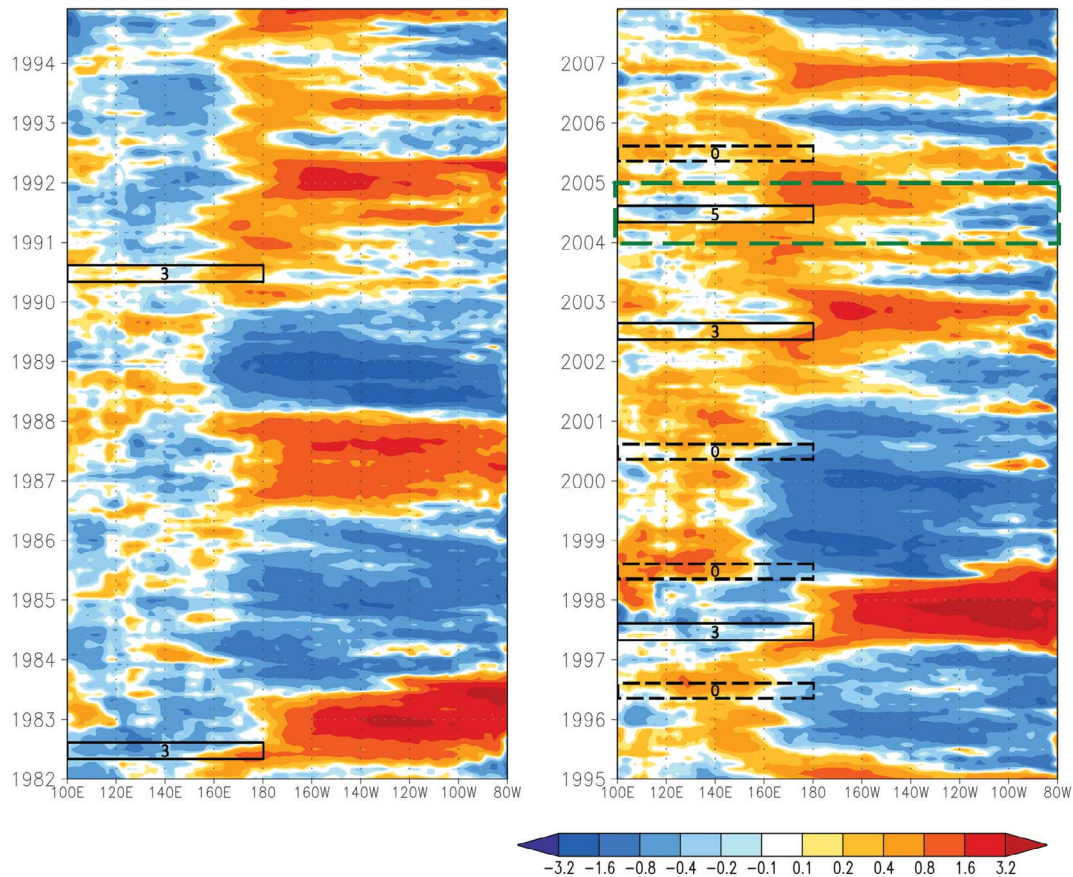
Figure 2. Hovmöller diagram of SST anomalies averaged from 5°S to 5°N. TC-active and TC-inactive events of June are shown by solid and dashed boxes, respectively, with the number of TC enclosed. The box drawn by green dashed line depicts the year of 2004, the focus of this study.

[15] Figure 2 is the Hovmöller diagram of the SSTA averaged from 5°S to 5°N. TC-active and TC-inactive months of June are shown by solid and dashed boxes, respectively. Among TC-active months of June, 1982–1983 and 1997–1998, were strong typical El Niño episodes, and the El Niño episode of 1991–1992 started from 1990. These El Niño episodes were accompanied by the warm SSTA in the central and eastern Pacific and the cold SSTA in the western Pacific, which began in summer of the developing year. Different from the typical El Niño events, the El Niño episodes of 2002–2003 and 2004–2005 had the warm SSTA in the central Pacific and the cold SSTAs in the eastern and western Pacific. These results indicate that all TC-active months of June were in the developing stage of El Niño episodes with the warm SSTA in the central Pacific and the cold SSTA in the western Pacific. In contrast, all TC-inactive months of June were in the developing stage or the mature stage of La Niña episodes (1995–1997, 1998–2002, and 2005–2006) during which a reversed SST distribution was present with the warm SSTA in the western Pacific and the cold SSTAs in the eastern Pacific and central Pacific.

[16] We examine the influence of the SST distribution on the circulation. The 25-year-averaged SST in June (Figure 3) shows a broad warm pool with SST greater than 29°C over the tropical WNP, and the cold SST at the equatorial eastern Pacific with coldest temperature lower than 24°C extending into the central Pacific along the equator. The easterly trade winds prevail over the central and eastern Pacific east of 150°E, while the westerlies exist west of 120°E between 5°N and 20°N. The easterly and westerly converge near the Philippines and turn into the southerly. Green dots in Figure 3 indicate the locations of TC genesis in June from 1982 to 2006. It is distributed in the southwest periphery of the NPSH. Note that the climatological monsoon westerly flow confined in the South China Sea (SCS) is not favorable for TC formation in the WNP.

[17] Further composites of the SST and wind at 850 hPa in June for TC-active, TC-inactive, TC-normal, El Niño developing, and La Niña years are performed to compare with those fields in June 2004. The results are shown in Figure 4. The composite fields for TC-active years (Figure 4a) show the warm (cold) SSTA in the tropics east (west) of 150°E, westerly anomalies in the WNP, and a large-scale cyclonic circulation anomaly north of the westerly anomaly. The large-scale flow provides a favorable condition for TC genesis (mean TC formation 3.4). Easterly vertical wind shear resides in the SCS and tropical northwestern Pacific west of 170°E. Most TCs preferentially develop near the zero shear line or in the easterly wind shear region. The latter may reflect the theoretical argument that
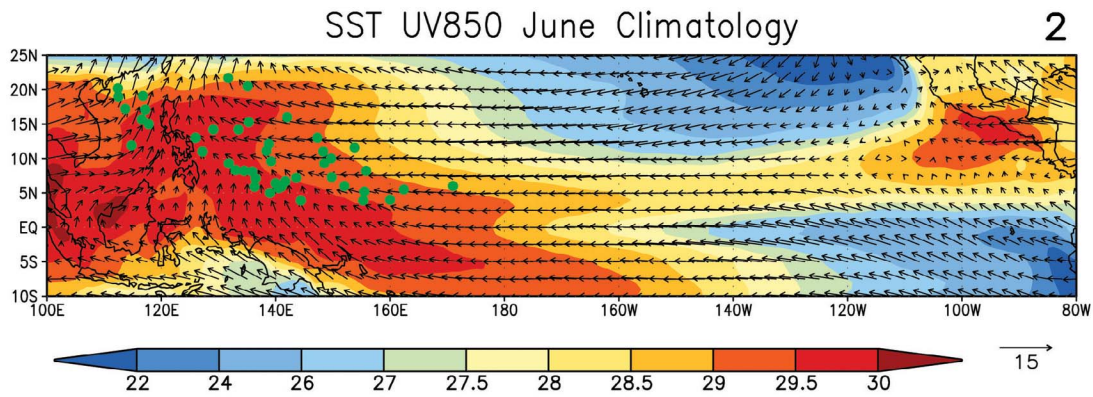
Figure 3. Winds (850 hPa) and SST in June averaged from 1982 to 2006. All TC genesis locations are indicated by green dots. The mean number of TCs formed in June is listed in the upper right corner (2).

the easterly wind shear may impact the development of low-level disturbances [*Xie and Wang*, 1996; *Ge et al.*, 2007]. The composite fields for TC-inactive years (Figure 4b) show reversed distribution with the warm (cold) SSTA located west (east) of 150°E and the easterly anomaly along the equator. The zone of the easterly vertical shear is shifted westward to the SCS and northward to the Philippine Sea. The large-scale anticyclonic circulation anomaly north of the equatorial easterly in the WNP is unfavorable for TC genesis (mean TC formation 0). The composite fields for years of normal TCs are shown in Figure 4c. Here the composite fields of the SSTA and wind anomalies are weak, meaning that they are similar to the climatological mean fields. The mean number of TC genesis (1.8) is also

similar to the climatological value of TCs in June (2). The zone of the easterly vertical wind shear extends to 160°E, which is similar to the climatological mean wind shear (figure not show). The composite fields for developing El Niño and La Niña conditions are shown in Figures 4d and 4e, and the corresponding mean TC genesis numbers are 2.6 and 1.2, respectively. They resemble the composite fields for TC-active and TC-inactive years shown in Figures 4a and 4b, respectively. In addition to the effect on genesis numbers, the developing warm events also cause an eastward extension of TC genesis locations as noted in previous studies.

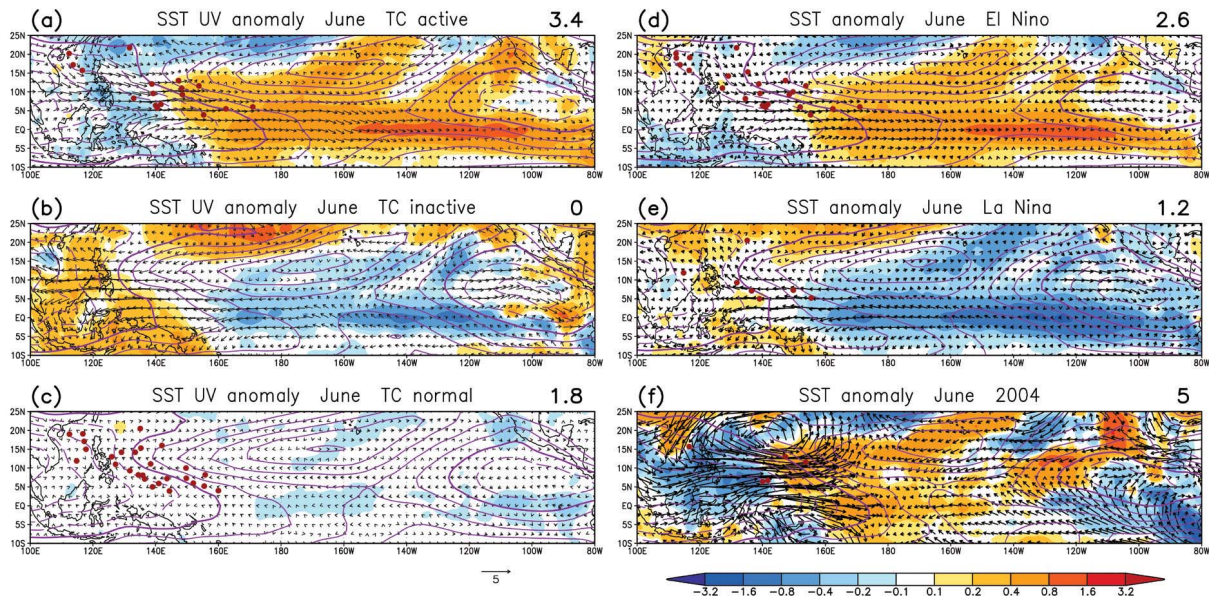[18] The SSTA and wind anomalies in June 2004 are shown in Figure 4f. Though it is similar to the composite

Figure 4. Same as Figure 3, but for anomaly fields in (a) TC-active categories (1982, 1990, 1997, 2002, and 2004), (b) TC-inactive categories (1996, 1998, 2000, and 2005), (c) normal categories (1983, 1984, 1985, 1986, 1987, 1988, 1989, 1991, 1992, 1993, 1994, 1995, 1999, 2001, 2003, and 2006), (d) El Niño episodes, (e) La Niña episodes, and (f) 2004. Dark red dots represent TC genesis positions. Solid (dashed) purple contours describe westerly (easterly) wind shear with the interval 5 m s^{-1}. Thick purple lines are the zero line of vertical shear.
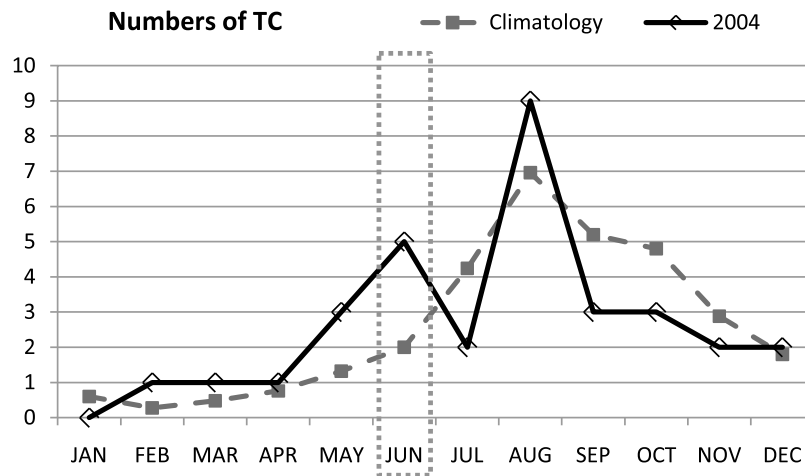
Figure 5. Number of TCs formed in each calendar month in the WNP. The dashed line denotes the average number from 1982 to 2006. The solid line is the number in 2004.

distribution of TC-active years and El Niño episodes, the SSTA fields have colder values west of 140°E and warmer values east of 140°E, resulting a stronger zonal gradient. The accompanying flow fields show stronger equatorial westerly anomaly and twin cyclonic circulation anomaly in western Pacific. What caused such a strong and favorable background condition for high TC activity in June 2004? We will investigate the role of the MJO and tropical waves in sections 4 and 5.

4. Modulation by the MJO

[19] The annual number of TC formation in 2004 is similar to the climatological mean number, but the number of TC formation shows a large month to month variation as revealed in Figure 5. Figure 5 shows more TCs in May, June, and August, and less TCs in July, September, and October than the corresponding climatological values. Such an intermonth variation is well correlated with intraseasonal oscillations as shown by the Hovmöller diagram of the unfiltered OLR (shading) and the space-time-filtered OLR at the MJO band (contours) from mid-May to August in 2004 (Figure 6). The OLR fields are averaged from 5°S to 5°N. Negative OLR (dashed contours) areas correspond to the MJO convective phase. Dots represent the formation time and longitude of TCs. Two major MJOs occurred during this season. Most TCs formed in the convective regions of the MJOs. In early May, three TCs formed behind the weak equatorial convective phase of the MJO. But within the following suppressed phase of the MJO in late May, no TC genesis was found. After the MJO suppressed phase, a strong MJO convective phase started from early June. It propagated to the east of the international date line and persisted until late June. Five TCs formed during this strong convective phase. The names, genesis locations and times, and the tracks of the five TCs are shown in Table 1 and Figure 7. The second suppressed phase of the MJO propagated eastward from the SCS in late June. It reached 160°W in mid-July with a TC formed at 130°E. Another strong convective phase occurred from mid-July to mid-August. This convective phase was longer than the MJO-
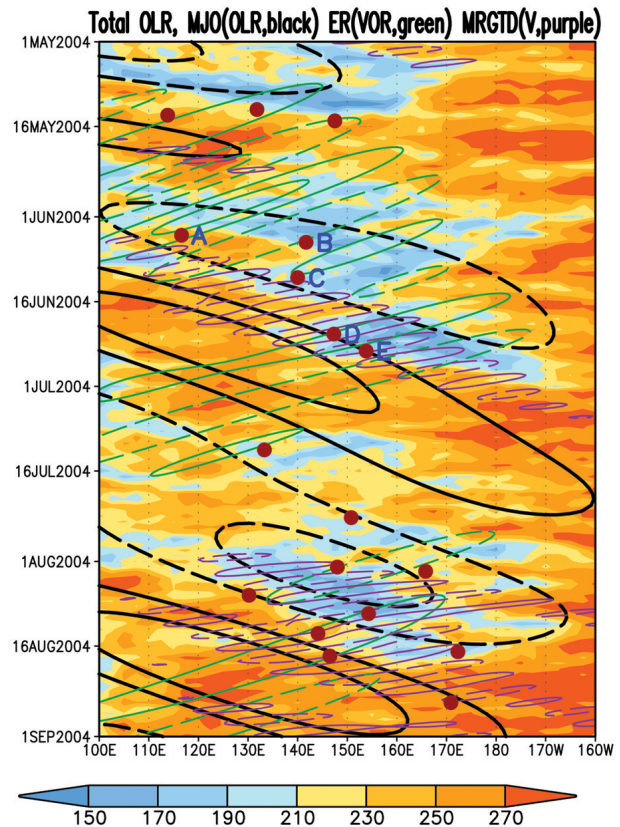

Figure 6. Hovmöller diagram of the unfiltered OLR (shaded) and the space-time-filtered OLR for MJO (black contours, interval 10 W m^{-1}) averaged from 5°S to 5°N. The period is from 1 May to 1 September 2004. Green and purple contours indicate the filtered vorticity and the meridional winds at 850 hPa for n = 1 Rossby waves and MRG-TD waves, respectively, averaged from 5°N to 15°N. The corresponding interval is 3×10^{-5} s^{-1} and 1.5 m s^{-1}. Solid (dashed) contours represent positive (negative) anomalies. Dots indicate the formation longitude and time of tropical cyclones.

Table 1. Tropical Cyclones That Occurred in WNP in June 2004 Based on Best Track Data From Joint Typhoon Warning Center

TC	Name	Warning Location	Warning Time
A	Conson	15.7°N, 116.6°E	0600 UT 4 June
B	Chanthu	6.7°N, 141.7°E	1200 UT 5 June
C	Dianmu	6.4°N, 140.0°E	1800 UT 11 June
D	Mindulle	13.0°N, 147.3°E	1800 UT 21 June
E	Tingting	11.6°N, 153.8°E	1800 UT 24 June

convective phase in June. Seven TCs occurred near the convective region in August. The MJO signal weakened after August.

[20] According to the RMM index, we define the monthly MJO events in each June as active or inactive. Eight of them are MJO-active events (1982, 1984, 1985, 1986, 1987, 1991, 2002, and 2004; see Figure 1). At least two or more TCs formed in all MJO-active events except 1991. Three MJO-active events corresponded with TC-active events. It shows that the MJO-active phase favors TC genesis. On the other hand among the seven MJO-inactive events (1988, 1995, 1996, 1997, 2003, 2005, and 2006), one had three TCs (1997), four had two TCs (1988, 1995, 2003, 2006), and two had no TC formation (1996, 2005), indicating no clear reduction in TC genesis in the MJO-inactive period.

[21] Considering the MJO and ENSO together, three MJO-active events were in the developing stage of El Niño episodes (1982, 2002, and 2004). These three events were also TC-active events. When multiscale climate oscillations form an in-phase large-scale condition, it is conducive to more TC genesis. The year 1997 was an MJO-inactive event, but it was in a developing stage of a strong El Niño episode. It became a TC-active event due to the contribution of the strong El Niño episode. On the other hand, in unfavorable climate conditions like the inactive MJOs and developing La Niña epi-

sodes (1988 and 1995), TC activities may still be above normal (e.g., two TCs formed in June 1988 and 1995). This indicates other important contribution factors to TC genesis, like submonthly-scale oscillations [*Fukutomi and Yasunari*, 1999; *Ko and Hsu*, 2006; *Chen and Sui*, 2010], Rossby wave energy dispersion in the wake of a preexisting TC [*Briegel and Frank*, 1997; *Ritchie and Holland*, 1999; *Sobel and Bretherton*, 1999; *Li et al.*, 2003; *Li and Fu*, 2006], mixed Rossby-gravity (MRG) waves within a monsoon confluent region [*Sobel and Bretherton*, 1999; *Kuo et al.*, 2001; *Dickinson and Molinari*, 2002; *Aiyyer and Molinari*, 2003], or synoptic scale (3–10 days) TD-type disturbances [*Lau and Lau*, 1990; *Takayabu and Nitta*, 1993; *Chang et al.*, 1996].

[22] For the 25 months of June from 1982 to 2006, total 268 days with 28 TCs fell in the MJO convective phase (5, 6, 7). On average, 3.13 TCs formed per month, similar to the average of TC-active Junes. On the other hand, total 303 days with 12 TCs fell in the MJO suppressed phase (1, 2, 3) for 25 Junes, resulting in the mean of 1.19 TCs. The result indicates that TC genesis is related to the MJO phase [*Liebmann et al.*, 1994; *Maloney and Hartmann*, 2000a, 2000b; *Kim et al.*, 2008]. We combined the filtered OLR fields for 268 days in the MJO convective phase, which showed a large negative OLR anomaly between the equator and 20°N over the WNP (Figure 8a). A large-scale westerly and cyclonic circulation anomalies were shown in companion with the tropical deep convection of the MJO system, providing a favorable environment for TC genesis. The opposite is true for the MJO suppressed phase (Figure 8b). The mean circulation and OLR for the MJO convective phase versus suppressed phase reveals a favorable condition for TC genesis by the MJO. This can further explain more TC formation in the MJO active phase in June. But it is inconsequential that less TCs formed when the MJO is inactive in June. However,
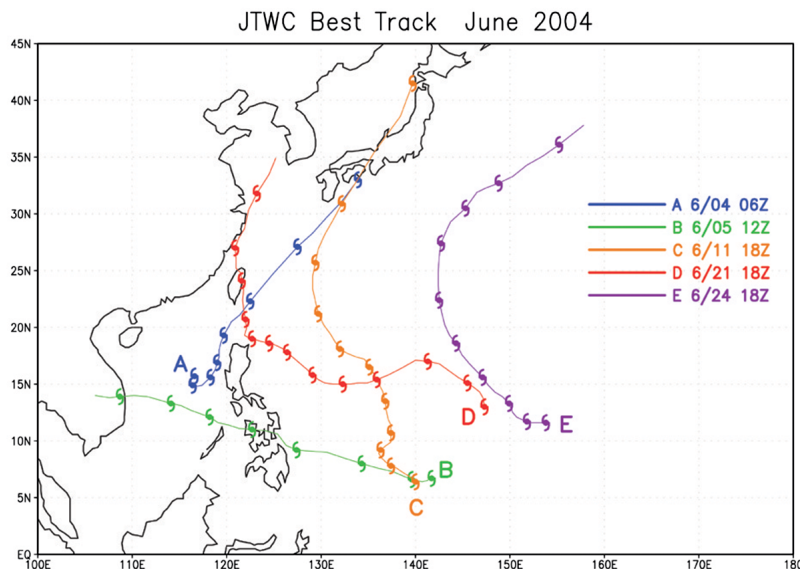

Figure 7. The Joint Typhoon Warning Center (JTWC) best tracks of the five TCs formed in WNP in June 2004. The sequence of genesis events is from A to E. The formation time for each TC is labeled to the right of the tracks. Each of the typhoon symbols along the tracks represents the TC centers every 24 h.
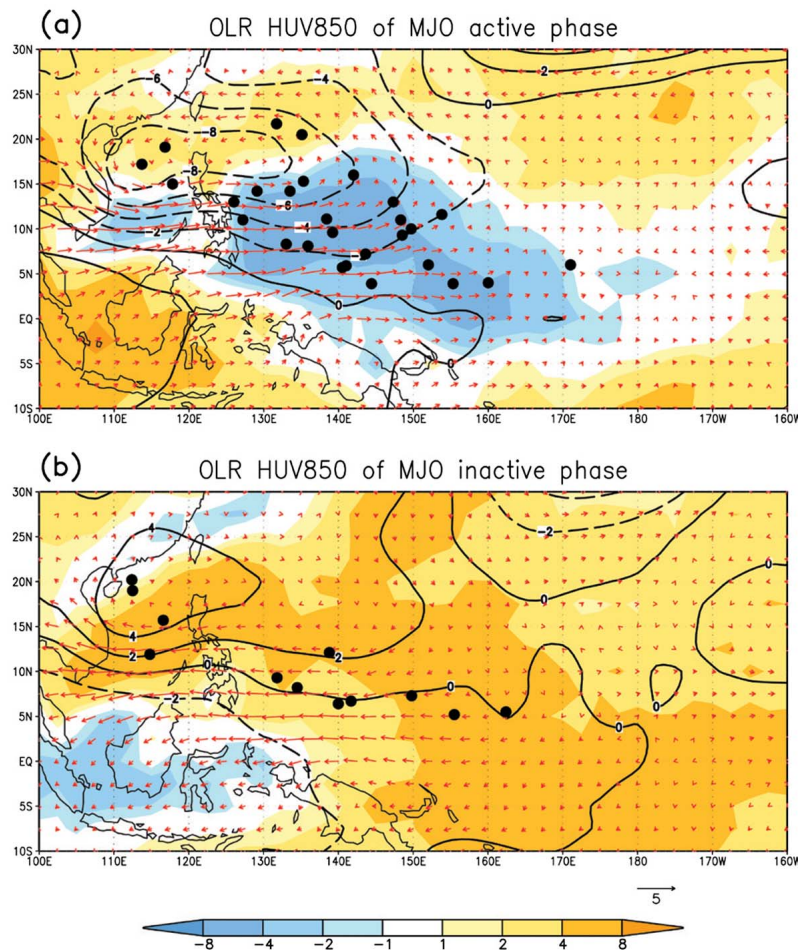
Figure 8. Composite fields of filtered OLR, geopotential height, and wind fields at 850 hPa for (a) MJO convective phase and (b) MJO suppressed phase in June from 1982 to 2006. Dots indicate the formation locations of tropical cyclones.

when the MJO is inactive, TC still occurs by other possible mechanisms as discussed above.

5. Tropical Waves and Their Relation With the MJO and TCs in June 2004

5.1. Evolution and Structure of Rossby Wave

[23] In addition to the favorable environmental conditions provided by El Niño and the MJO-active phase, tropical waves were also active during 2004 warm season. We showed in Figure 6, the 850 hPa relative vorticity of the Rossby wave and the 850 hPa meridional wind of the MRG-TD type wave disturbances averaged within 5°N–15°N. These tropical waves are extracted by space-time filtering as discussed in section 2. In Figure 6, a group of Rossby waves occurred in the SCS from May. The wave disturbances of the Rossby waves emerged and grew in the east and decayed in the west. While the developed disturbances traveled westward, new disturbances emerged east of the existing disturbances. Such an eastward development of new wave genesis is a result of Rossby waves (energy) dispersion. For such an energy dispersion to sustain, waves of different wavelength must be excited first by the large-scale cyclonic flow associated with the MJO heating and developing El Niño, and be

maintained either by diabatic heating (wave-convection coupling) or by energy conversion from mean available potential energy to eddy available potential energy in the presence of mean vertical shear [*Xie and Wang*, 1996]. Such a consideration of wave genesis and development leads us to suggest that the evolution of Rossby waves in May was influenced by the MJO occurred in early May, whereas the Rossby waves in June were influenced by the following MJO developed through June. Four of five TCs in June occurred near the positive vorticity region of the Rossby wave. The Rossby waves developed in late June near the dateline were long-lived through mid-July when the western equatorial Pacific was in the MJO-inactive phase. Another MJO developed in August but only one positive vorticity center existed in August, and three TCs formed near the convective region during this period.

[24] The horizontal structure of the convectively coupled Rossby wave is revealed by the circulation and OLR fields at the 850 hPa level at 4 June 2004 in Figure 9. The 850 hPa circulations are generally like that of the theoretical shallow water $n = 1$ Rossby wave except that the Northern Hemisphere components are tilted eastward with increasing latitude. The maximum amplitude of the wave trains is located near 10°N. The predominant zonal wave number of the circulation at this level is around 4 to 5, similar to the
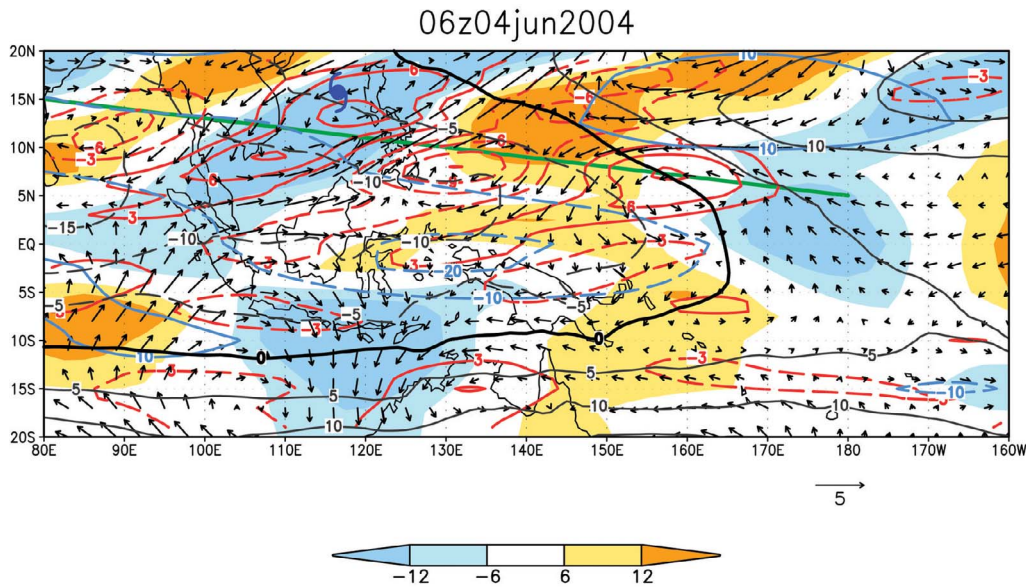
Figure 9. The horizontal structure of Rossby wave at TC A genesis time: OLR (color shaded), vorticity at 850 hPa (red contours, interval 3×10^{-5} s^{-1}), and horizontal winds at 850 hPa. The MJO is also shown by OLR (blue contours, interval 10 W m^{-1}, zero line skipped). Black contours describe the monthly mean zonal vertical shear with the interval 5 m s^{-1}. The blue Typhoon mark indicates the genesis location of TC A. Green line is the track for vertical cross section shown in Figure 10.

observed features of n = 1 equatorial Rossby waves documented by *Wheeler et al.* [2000]. The enhanced convection occurs in the region where the 850 hPa convergence occurs in the Southern Hemisphere (not shown), but it is shifted and tilted to be in phase with the elongated cyclonic vorticity center in the Northern Hemisphere. The wave structure in the Northern Hemisphere shown in Figure 9 resembles the observed features of quasi-biweekly oscillations (QBWO) over the WNP during boreal summer reported by *Chen and Sui* [2010]. The observed wave structure also agrees with the theoretical features of the unstable Rossby wave in the presence of easterly vertical shear shown by *Xie and Wang* [1996] and *Chatterjee and Goswami* [2004]. The vertical structure along the Rossby wave train is shown in Figure 10. Easterly vertical shear existed west of 145°E, where low-level divergence (convergence) was collocated with anticyclonic (cyclonic) vorticity center. The vertical structure tilted westward with height. In contrast, low-level convergence (divergence) was located to the east of the positive (negative) vorticity anomalies in westerly vertical shear (east of 145°E) where the vertical tilt was not evident. In the easterly vertical shear, convection is more strongly coupled with the rotational winds in the lower troposphere such that the waves are unstable. This is consistent with the heat budget analysis of the QBWO described by *Chen and Sui* [2010] who found that diabatic heating in the tropics is the most dominant term in the generation of EAPE. In the westerly vertical shear, convection is relatively less dominant in the evolution of Rossby waves so the wave structure is similar to the theoretical stable Rossby wave with low-level convergence located to the east of the positive vorticity anomalies for about 1/4–1/8 of a wavelength. This is also consistent with the finding of *Chen and Sui* [2010] that the QBWO can be traced to equatorially trapped n = 1 Rossby mode.

5.2. MRG-TD Wave Structure

[25] The series of MRG-TD waves were developed in early June from the SCS (Figure 6) behind the equatorial convective region of the MJO. Two TCs formed near the convective zone of the MRG-TD wave series in late June. Another organized MRG-TD wave series occurred in early August and crossed the date line in late August, coinciding with the second strong MJO convective phase. The two MRG wave packets were phase locked to the MJO evolution. The group speed of the MRG-TD wave train (about 4.2 m s^{-1}) was eastward and was similar to the eastward phase speed of the MJO (about 4.5 m s^{-1}). A close examination of Figure 6 reveals that the MRG-TD disturbances in early and mid June 2004 moved westward at speed of 5.9 m s^{-1}, which is slower than the waves in late June that moved at speed of 9 ms^{-1}. The corresponding wave structure is also different as shown by the horizontal circulation at 850 hPa and OLR fields at 11 and 24 June in Figures 11a and 11b, respectively. The circulation in 11 June shows a northwest-southeast elongated wave pattern emanating from the region near (140°E, 5°N) where TC C was formed. The features of the wave train (wavelength 3800 km, northwestward propagation, period 7.5 days) are similar to those found by *Lau and Lau* [1990] and *Chang et al.* [1996]. Such TD-type disturbances occurred in the monsoon trough where wave accumulation causes scale contraction and wave amplification by barotropic conversion [*Sobel and Bretherton*, 1999; *Kuo et al.*, 2001]. In the case of 24 June when the MJO suppressed phase moved to the WNP where vertical wind shear was weak, the MRG-TD wave structure (Figure 11b) is similar to the theoretical MRG wave structure [*Matsuno*, 1966]. The MRG-TD wave propagated northwestward and transformed to off-equatorial TD-type disturbance. Four of
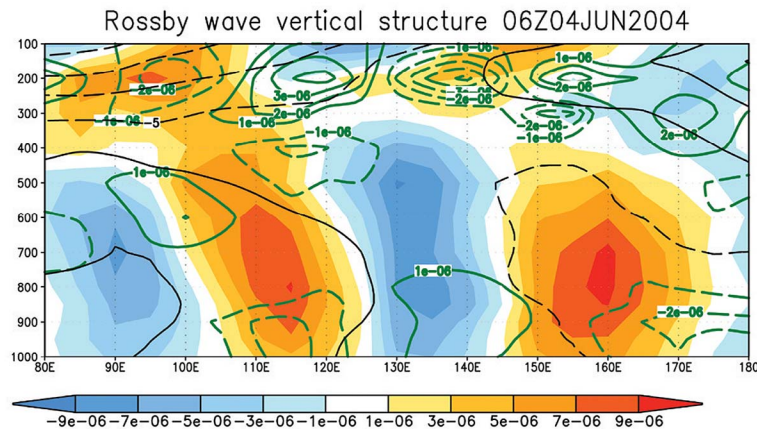
Figure 10. The vertical structure of Rossby wave along the track shown in Figure 9 at TC A genesis time: vorticity (color shaded), divergence (green contours), and zonal wind (black contours) averaged within 5° longitude along the cross section of the total wind field with the interval 5 m s^{-1}.
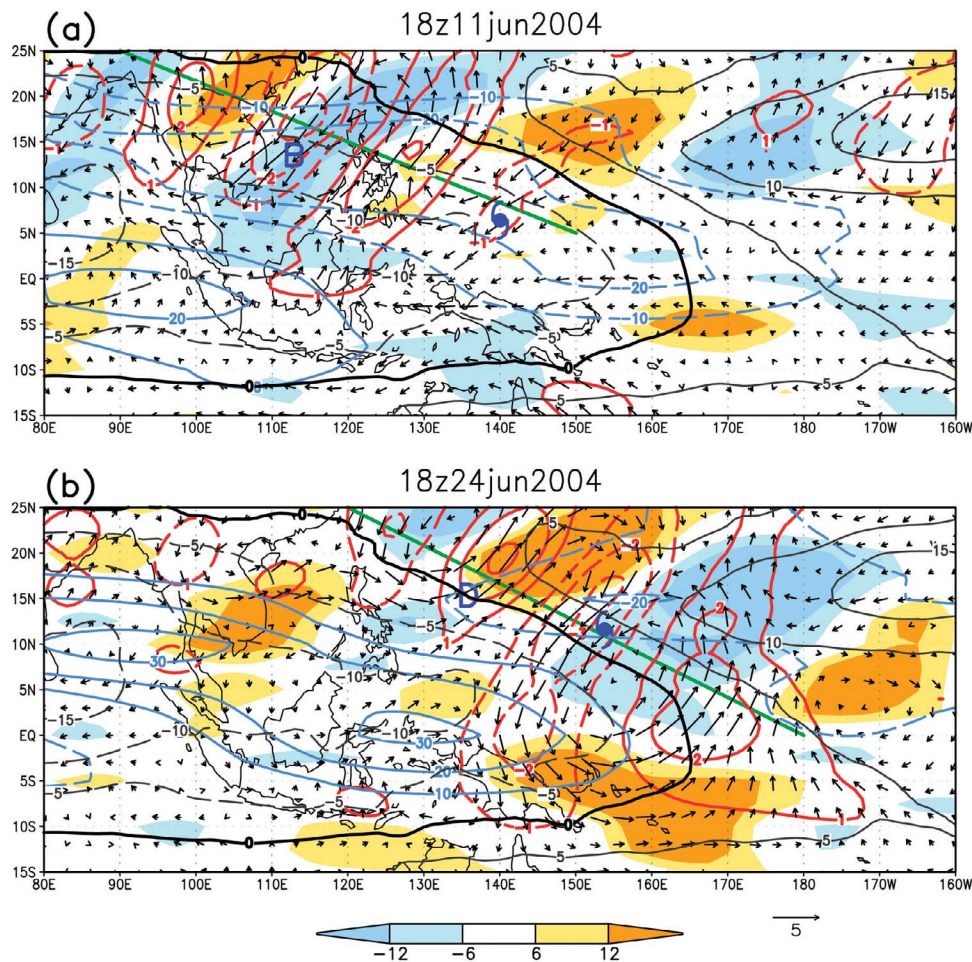

Figure 11. Same as Figure 9, but for MRG-TD wave at (a) TC C and (b) TC E genesis time. The meridional wind fields at 850 hPa in shown in red contours (interval 1 m s^{-1}). The blue typhoon marks indicate the genesis location of TC C and TC E. Mark B and D indicate the location of TC B and TC D, respectively, at TC C genesis time. The green line in Figures 11a and 11b is the track for vertical cross section shown in Figures 12a and 12b, respectively.
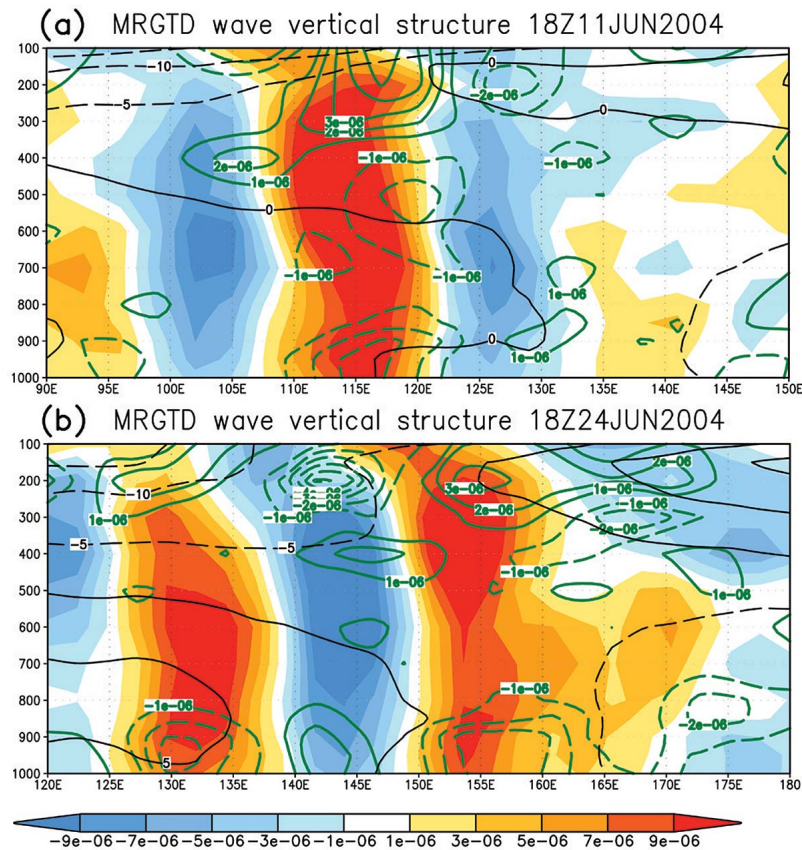
Figure 12. Same as Figure 10 but for MRG-TD wave at (a) TC C and (b) TC E genesis time (see Figure 11 for orientation).

the five TCs (TC B, C, D, and E) are found to be associated with the MRG-TD waves shown in Figure 11. Figures 12a and 12b show the vertical structure at 11 and 24 June, respectively. As shown in Figure 10, the low-level divergence (convergence) coincided with the negative (positive) vorticity center. In addition, the vertical structure was tilted westward in easterly vertical shear. In westerly vertical shear region, eastern portion of the wave train, low-level convergence lagged behind the vorticity center for about 1/4–1/8 of a wavelength. These contrasting features are consistent with the features of tropical summertime synoptic-scale waves shown by *Tam and Li* [2006]. They suggested that the circulation east of ~150°E is governed by adiabatic dynamics, but rising motion is more related to convection to the west.

5.3. Quantitative Contribution

[26] Figure 6 provides a qualitative description of TC formation in different large-scale wave disturbances. The first TC in June (TC A) was related by both the MJO and Rossby wave. The second TC (TC B) formed near the convective region of the MJO, but in a suppressed region of Rossby wave. The third TC (TC C) formed near the core of the convective region of the MJO, east of a convective region of Rossby wave. The genesis of the fourth and fifth TCs (TCs D and E) appears to be related to the MJO, Rossby wave and MRG-TD wave all.

[27] To further quantify the possible effect of tropical waves on TC formation, we calculated the percentage of

vorticity of each wave (Table 2) relative to the total vorticity at the genesis time and location. The Rossby wave was more than three fourths of total vorticity when TC A was formed. The second related wave of TC A formation was the MJO, which was about 12%. TC B formation was mainly related to the MJO, which was 22% of total vorticity. The main related wave to TC C formation was the Rossby wave. The percentage was 11.2. The MJO was the main related wave to TC D formation with 10.3%. The MRG-TD wave was about one third of total vorticity for TC E formation. The second related wave to TC A was the MJO with 15.4%.

[28] The percentage analysis is easy and quick to distinguish the main wave related to TC formation. However, the inconsistent denominators of TCs could confound the relation of waves. For example, the percentage of MJO in TC A was larger than the percentage of the MJO in TC D, but the

Table 2. Percentage of Vorticity for Three Tropical Wave Disturbances (MJO, ER, and MRG-TD) to Total Vorticity at 850 hPa at TC Warning Time of the Five TCs[a]

TC	MJO	ER	MRG-TD
A	12.9	**76.5**	−16.1
B	**22.0**	7.1	5.3
C	2.9	**11.2**	3.2
D	**10.3**	5.5	4.3
E	15.4	8.0	**30.9**

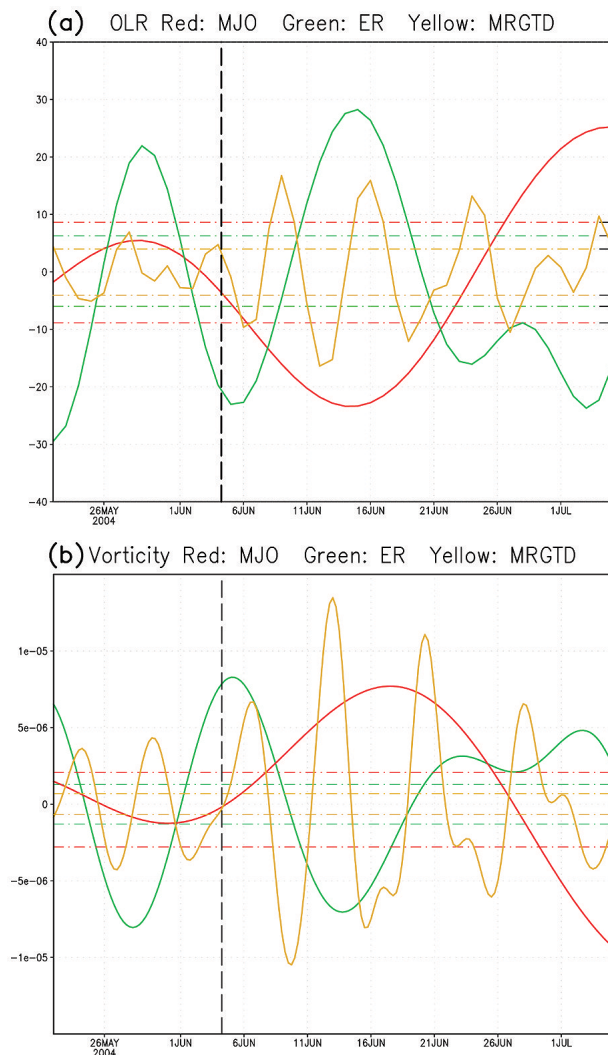[a]The largest percentages of TCs are denoted in boldface.

Figure 13. Time series of (a) OLR and (b) vorticity at the genesis location of TC A. The values of MJO, Rossby wave, and MRG-TD wave are shown by red, green, and yellow lines, respectively. Vertical black dashed lines describe the time of TC formation. Dash-dotted lines indicate the range of 1 standard deviation of each wave.

MJO was the main related wave to TC D formation. That is because the total vorticity of TC D was larger than TC A. In order to reduce the inconsistent effect of the denominators, we analyzed the evolution of each wave at the location of

TC formation. Figure 13 shows the time series of OLR and vorticity fields in June at TC A genesis location. At the time of TC A genesis, the variation of Rossby wave was larger than one standard deviation. Rossby wave was the most significantly related wave for TC A formation in terms of both OLR and vorticity fields. The variation of the MJO also exceeded one standard deviation in OLR field. However, the variation of the MJO in vorticity field and the variation of MRG-TD wave in OLR and vorticity fields were insignificant at the genesis time of TC A.

[29] To consider the contribution by both vorticity and divergence fields, we simply compute the sum of the normalized OLR and vorticity as a wave related (WR) index. Table 3 shows the normalized values of OLR, vorticity, and the sum of the two. The largest normalized OLR and vorticity of TC A formation were all from Rossby wave. The normalized OLR and vorticity of the MJO and MRG-TD wave were small and three of them were negative. The WR index shows that Rossby wave was the main wave related to TC A genesis. Unlike TC A, the largest normalized OLR and vorticity in TC B formation were from different waves. The MJO had the largest normalized OLR and the second largest normalized vorticity. The Rossby wave had the largest normalized vorticity, but negative normalized OLR. The WR index of the MJO was the largest in TC B formation. The normalized OLR associated with the MJO and Rossby wave had comparable values at the genesis time of TC C. Rossby wave had the largest normalized vorticity, which was 2.8 times the value of the MJO. The WR index shows the main wave related to TC C formation was Rossby wave. TC D formed in a complex environment. The largest normalized OLR in TC D formation was the MJO, though all the normalized vorticity of three waves exceeded three. The difference in normalized vorticity and WR index between three waves were less than one. This result shows that all of three waves were active when TC D formed. In TC E formation stage, the MRG-TD wave had the largest normalized OLR and vorticity. The large value of the normalized vorticity indicates that the MRG-TD wave dominated when TC E formed. The same result is shown in WR index. The results of WR index were consistent with the result of fractional vorticity analysis. Except TC A, the value of WR index for the MJO all exceeded 2.5. It shows that most TCs are related to the arrival of active MJO envelope to the WNP. Even for TC A, the MJO still plays a positive role. The MJO contributed a favorable background state for TC genesis and high-frequency wave activity. The high-frequency waves, like MRG-TD wave, could be associated with TCs. It also may be

Table 3. Normalized OLR and Vorticity at 850 hPa and the Wave-Related (WR) Index for the Three Tropical Wave Disturbances (MJO, ER, and MRG-TD) at TC Warning Time of the Five TCs[a]

TC	OLR			Vorticity			WR Index		
	MJO	Rossby	MRG-TD	MJO	Rossby	MRG-TD	MJO	Rossby	MRG-TD
A	0.34	**3.21**	−1.18	−0.08	**6.08**	−0.45	0.26	**9.29**	−1.63
B	**1.04**	−1.66	0.28	1.49	**1.87**	1.14	**2.53**	0.21	1.42
C	**2.44**	2.26	−0.21	1.44	**4.06**	3.07	3.88	**6.32**	2.86
D	**2.70**	1.42	1.22	3.02	**3.79**	3.66	**5.72**	5.21	4.88
E	1.68	2.14	**2.43**	2.15	2.75	**13.46**	3.83	4.89	**15.89**

[a]Boldface indicates the main related wave to TC formation.

a part of the low-frequency ISO convective system [*Straub and Kiladis*, 2003].

6. Summary and Discussion

[30] June is a transition month from an unfavorable condition to a favorable condition for TC formation. Tropical cyclogenesis in June is more sensitive to favorable large-scale conditions. The month of June in 2004 was a month of active tropical waves, a strong MJO in western Pacific warm pool, along with a developing warm (El Niño) episode. Five TCs formed in this particular month and were related to the active multiscale wave variations. Analyzing this unusual month helps to clarify the role of multiscale wave variations in tropical cyclogenesis. Part 1 of this study examines the climate background of the unusual event and identify the main wave related to TC formation. The detail investigation of the relationship between the multiscale wave variation and TC formation will be considered in a future companion paper.

[31] Our analysis reveals that the composite fields for TC-active (TC-inactive) months of June resembled that of the developing stage of an El Niño (La Niña) episode. This indicates a dominant role played by long-term SST variations in the tropical central Pacific and westerly wind anomalies associated with the monsoon trough that provides a favorable large-scale circulation for TC genesis. It also created a cyclonic circulation anomaly in the WNP. The SSTA and low-level winds in June 2004 are quite similar to the June composite of TC-active events but of much stronger amplitudes.

[32] Analyzing the number of TC genesis corresponding to the phase of the MJO, tropical deep convection associated with the MJO convective (suppressed) phase accompanied a large-scale low-level cyclonic (anticyclonic) circulation anomaly in the WNP. The cyclonic circulation anomaly provided a favorable condition for TC genesis in June and more TCs tended to form. In the MJO suppressed phase, the number of TC formation may still be above normal because of other favorable conditions. The high TC genesis in June 2004 is a combined result of a favorable large-scale environment provided by a developing El Niño warming condition and an unusually strong MJO event that is coupled with high tropical waves-TC activities.

[33] We further examined the Rossby waves and MRG-TD disturbances in relation to the MJO evolution. The results indicate that the series of Rossby waves originated in May, June, and early August 2004 were all related to corresponding MJOs. An even closer link is found between the MRG-TD disturbances and MJOs. The wave structure of the Rossby waves is generally consistent with the unstable n = 1 Rossby waves in the mean flow with easterly vertical shear. The MRG-TD type disturbances show two distinct wave structures. The structure for those developed in the monsoon trough region west of 160°E resemble that of the summertime synoptic-scale (TD-type) disturbance found in previous studies. The structure for those developed east of 160°E is similar to the theoretical MRG waves which propagate northwestward and transform into TD-type disturbances.

[34] We also defined a WR index by adding normalized OLR and vorticity at 850hPa to quantify the relative importance of waves to TC formation. In June 2004, the main wave related to TC A and TC C formation was Rossby wave. The MJO was the most related to TC B and TC D formation. MRG-TD wave was the main wave related to TC E formation. Some TC formation was related to more than one wave.

[35] The large-scale background analysis of June 2004 shows a favorable environment for TC genesis established by a developing El Niño episode and an active MJO. These results suggest that the MJO heating and the large-scale cyclonic flow in the lower troposphere provide important forcings for generating equatorial n = 1 Rossby waves and MRG-TD disturbances in the large-scale unstable environment (easterly vertical shear). The waves propagate westward or northwestward with an eastward energy dispersion in the presence of mean flow. TCs may have formed in the active phase of Rossby and MRG-TD waves. TCs may also play an active role in the generation and development of these waves. The waves-TC interaction will be reported in a future companion paper.

References

Aiyyer, A. R., and J. Molinari (2003), Evolution of mixed Rossby-gravity waves in idealized MJO environments, *J. Atmos. Sci.*, *60*, 2837–2855, doi:10.1175/1520-0469(2003)060<2837:EOMRWI>2.0.CO;2.

Bessafi, M., and M. C. Wheeler (2006), Modulation of south Indian Ocean tropical cyclones by the Madden-Julian Oscillation and convectively coupled equatorial waves, *Mon. Weather Rev.*, *134*, 638–656, doi:10.1175/MWR3087.1.

Briegel, L. M., and W. M. Frank (1997), Large-scale influences on tropical cyclogenesis in the western North Pacific, *Mon. Weather Rev.*, *125*, 1397–1413, doi:10.1175/1520-0493(1997)125<1397:LSIOTC>2.0.CO;2.

Camargo, S. J., and A. H. Sobel (2005), Western North Pacific tropical cyclone intensity and ENSO, *J. Clim.*, *18*, 2996–3006, doi:10.1175/JCLI3457.1.

Chan, J. C. L. (2005), Interannual and interdecadal variations of tropical cyclone activity over the western North Pacific, *Meteorol. Atmos. Phys.*, *89*, 143–152, doi:10.1007/s00703-005-0126-y.

Chan, J. C. L., J. E. Shi, and C. M. Lam (1998), Seasonal forecasting of tropical cyclone activity over the western North Pacific and the South China Sea, *Weather Forecast.*, *13*, 997–1004, doi:10.1175/1520-0434(1998)013<0997:SFOTCA>2.0.CO;2.

Chang, C.-P., J. M. Chen, P. A. Harr, and L. E. Carr (1996), Northwest-ward-propagating wave patterns over the tropical western North Pacific during summer, *Mon. Weather Rev.*, *124*, 2245–2266, doi:10.1175/1520-0493(1996)124<2245:NPWPOT>2.0.CO;2.

Chatterjee, P., and B. N. Goswami (2004), Structure, genesis and scale selection of the tropical quasi-biweekly mode, *Q. J. R. Meteorol. Soc.*, *130*, 1171–1194, doi:10.1256/qj.03.133.

Chen, G., and R. H. Huang (2009), Interannual variation of the mixed Rossby-gravity waves and their impact on tropical cyclogenesis in the western North Pacific, *J. Clim.*, *22*, 535–549, doi:10.1175/2008JCLI2221.1.

Chen, G., and C.-H. Sui (2010), Characteristics and origin of quasi-biweekly oscillation over the western North Pacific during boreal summer, *J. Geophys. Res.*, *115*, D14113, doi:10.1029/2009JD013389.

Chen, T.-C., S.-Y. Wang, M.-C. Yen, and W. A. Gallus (2004), Role of the monsoon gyre in the interannual variation of tropical cyclone formation over the western North Pacific, *Weather Forecast.*, *19*, 776–785, doi:10.1175/1520-0434(2004)019<0776:ROTMGI>2.0.CO;2.

Chen, T.-C., S.-Y. Wang, and M.-C. Yen (2006), Interannual variation of the tropical cyclone activity over the western North Pacific, *J. Clim.*, *19*, 5709–5720, doi:10.1175/JCLI3934.1.

Chia, H. H., and C. F. Ropelewski (2002), The interannual variability in the genesis location of tropical cyclones in the northwest Pacific, *J. Clim.*, *15*, 2934–2944, doi:10.1175/1520-0442(2002)015<2934:TIVITG>2.0. CO;2.

Chu, J.-H., C. R. Sampson, A. S. Levine, and E. Fukada (2002), The Joint Typhoon Warning Center Tropical Cyclone Best-Tracks, 1945–2000, *NRL Ref. NRL/MR/7540-02-16*, Naval Res. Lab., Washington, D. C.

Chu, P.-S. (2004), ENSO and tropical cyclone activity, in *Hurricanes and Typhoons: Past, Present, and Potential*, edited by R. J. Murnane and K. B. Liu, pp. 297–332, Columbia Univ. Press, New York.

Dickinson, M., and J. Molinari (2002), Mixed Rossby-gravity waves and western Pacific tropical cyclogenesis. Part I: Synoptic evolution, *J. Atmos. Sci.*, *59*, 2183–2196, doi:10.1175/1520-0469(2002)059<2183: MRGWAW>2.0.CO;2.

Frank, W. M., and P. E. Roundy (2006), The role of tropical waves in tropical cyclogenesis, *Mon. Weather Rev.*, *134*, 2397–2417, doi:10.1175/ MWR3204.1.

Fukutomi, Y., and T. Yasunari (1999), 10–25 day intraseasonal variations of convection and circulation over East Asia and western North Pacific during early summer, *J. Meteorol. Soc. Jpn.*, *77*, 753–769.

Ge, X., T. Li, and X. Zhou (2007), Tropical cyclone energy dispersion under vertical shears, *Geophys. Res. Lett.*, *34*, L23807, doi:10.1029/ 2007GL031867.

Hall, J. D., A. J. Matthews, and D. J. Karoly (2001), The modulation of tropical cyclone activity in the Australian region by the Madden-Julian Oscillation, *Mon. Weather Rev.*, *129*, 2970–2982, doi:10.1175/1520-0493(2001)129<2970:TMOTCA>2.0.CO;2.

Harr, P. A. (2006), Temporal clustering of tropical cyclone occurrence on intraseasonal time scales, paper presented at 27th Conference on Hurricanes and Tropical Meteorology, Am. Meteorol. Soc., Monterey, Calif.

Ho, C.-H., J.-H. Kim, J.-H. Jeong, H.-S. Kim, and D. Chen (2006), Variation of tropical cyclone activity in the South Indian Ocean: El Niño–Southern Oscillation and Madden-Julian Oscillation effects, *J. Geophys. Res.*, *111*, D22101, doi:10.1029/2006JD007289.

Hsu, H.-H., C.-H. Hung, A.-K. Lo, and C.-W. Hung (2008), Influence of tropical cyclone on the estimation of climate variability in the tropical western North Pacific, *J. Clim.*, *21*, 2960–2975, doi:10.1175/ 2007JCLI1847.1.

Hsu, P.-C., C.-H. Tsou, H.-H. Hsu, and J.-H. Chen (2009), Eddy energy along the tropical storm track in association with ENSO, *J. Meteorol. Soc. Jpn.*, *87*, 687–704, doi:10.2151/jmsj.87.687.

Kanamitsu, M. (1989), Description of the NMC global data assimilation and forecast system, *Weather Forecast.*, *4*, 335–342, doi:10.1175/ 1520-0434(1989)004<0335:DOTNGD>2.0.CO;2.

Kanamitsu, M., W. Ebisuzaki, J. Woollen, S.-K. Yang, J. J. Hnilo, M. Fiorino, and G. L. Potter (2002), NCEP-ODE AMIP-II reanalysis (R-2), *Bull. Am. Meteorol. Soc.*, *83*, 1631–1643, doi:10.1175/BAMS-83-11-1631 (2002)083<1631:NAR>2.3.CO;2.

Kim, J.-H., C.-H. Ho, and C.-H. Sui (2005), Circulation features associated with the record-breaking typhoon landfall on Japan in 2004, *Geophys. Res. Lett.*, *32*, L14713, doi:10.1029/2005GL022494.

Kim, J.-H., C.-H. Ho, H.-S. Kim, C.-H. Sui, and S. K. Park (2008), Systematic variation of summertime tropical cyclone activity in the western North Pacific in relation to the Madden-Julian Oscillation, *J. Clim.*, *21*, 1171–1191, doi:10.1175/2007JCLI1493.1.

Ko, K.-C., and H.-H. Hsu (2006), Sub-monthly circulation features associated with tropical cyclone tracks over the East Asian monsoon area during July–August season, *J. Meteorol. Soc. Jpn.*, *84*, 871–889, doi:10.2151/ jmsj.84.871.

Ko, K.-C., and H.-H. Hsu (2009), ISO modulation on the submonthly wave pattern and recurving tropical cyclones in the tropical western North Pacific, *J. Clim.*, *22*, 582–599, doi:10.1175/2008JCLI2282.1.

Kuo, H.-C., J.-H. Chen, R. T. Williams, and C.-P. Chang (2001), Rossby waves in zonally opposing mean flow: Behavior in northwest Pacific summer monsoon, *J. Atmos. Sci.*, *58*, 1035–1050, doi:10.1175/1520-0469(2001)058<1035:RWIZOM>2.0.CO;2.

Landsea, C. W. (2000), El Niño–Southern Oscillation and the seasonal predictability of tropical cyclones, in *El Niño: Impacts of Multiscale Variability on Natural Ecosystems and Society*, edited by H. F. Diaz and V. Markgraf, pp. 149–181, Cambridge Univ. Press, Cambridge, U. K.

Lau, K.-H., and N.-C. Lau (1990), Observed structure and propagation characteristics of tropical summertime synoptic scale disturbances, *Mon. Weather Rev.*, *118*, 1888–1913, doi:10.1175/1520-0493(1990) 118<1888:OSAPCO>2.0.CO;2.

Lau, K.-H., and N.-C. Lau (1992), The energetics and propagation dynamics of tropical summertime synoptic-scale disturbances, *Mon. Weather Rev.*, *120*, 2523–2539, doi:10.1175/1520-0493(1992)120<2523:TEAP-DO>2.0.CO;2.

Li, T., and B. Fu (2006), Tropical cyclogenesis associated with Rossby wave energy dispersion of a preexisting typhoon. Part I: Satellite data analyses, *J. Atmos. Sci.*, *63*, 1377–1389, doi:10.1175/JAS3692.1.

Li, T., B. Fu, X. Ge, B. Wang, and M. Peng (2003), Satellite data analysis and numerical simulation of tropical cyclone formation, *Geophys. Res. Lett.*, *30*(21), 2122, doi:10.1029/2003GL018556.

Liebmann, B., and C. A. Smith (1996), Description of a complete (interpolated) outgoing longwave radiation dataset, *Bull. Am. Meteorol. Soc.*, *77*, 1275–1277.

Liebmann, B., H. H. Hendon, and J. D. Glick (1994), The relationship between tropical cyclones of the western Pacific and Indian oceans and the Madden-Julian Oscillation, *J. Meteorol. Soc. Jpn.*, *72*, 401–411.

Lindzen, R. D. (1967), Planetary waves on beta-planes, *Mon. Weather Rev.*, *95*, 441–451, doi:10.1175/1520-0493(1967)095<0441: PWOBP>2.3.CO;2.

Madden, R. A., and P. R. Julian (1971), Detection of a 40–50 day oscillation in the zonal wind in the tropical Pacific, *J. Atmos. Sci.*, *28*, 702–708, doi:10.1175/1520-0469(1971)028<0702:DOADOI>2.0.CO;2.

Maloney, E. D., and M. J. Dickinson (2003), The intraseasonal oscillation and the energetics of summertime tropical western North Pacific synoptic-scale disturbances, *J. Atmos. Sci.*, *60*, 2153–2168, doi:10.1175/1520-0469(2003)060<2153:TIOATE>2.0.CO;2.

Maloney, E. D., and D. L. Hartmann (2000a), Modulation of hurricane activity in the Gulf of Mexico by the Madden-Julian Oscillation, *Science*, *287*, 2002–2004, doi:10.1126/science.287.5460.2002.

Maloney, E. D., and D. L. Hartmann (2000b), Modulation of eastern North Pacific hurricane by the Madden-Julian Oscillation, *J. Atmos. Sci.*, *13*, 1451–1460.

Maloney, E. D., and D. L. Hartmann (2001), The Madden-Julian Oscillation, barotropic dynamics, and North Pacific tropical cyclone formation. Part I: Observations, *J. Atmos. Sci.*, *58*, 2545–2558, doi:10.1175/1520-0469(2001)058<2545:TMJOBD>2.0.CO;2.

Matsuno, T. (1966), Quasi-geostrophic motions in the equatorial area, *J. Meteorol. Soc. Jpn.*, *44*, 25–43.

Molinari, J., and D. Vollaro (2000), Planetary- and synoptic-scale influences on eastern Pacific tropical cyclogenesis, *Mon. Weather Rev.*, *128*, 3296–3307, doi:10.1175/1520-0493(2000)128<3296:PASSIO>2.0. CO;2.

Molinari, J., D. Knight, M. Dickinson, D. Vollaro, and S. Skubis (1997), Potential vorticity, easterly waves, and eastern Pacific tropical cyclogenesis, *Mon. Weather Rev.*, *125*, 2699–2708, doi:10.1175/1520-0493(1997) 125<2699:PVEWAE>2.0.CO;2.

Nakazawa, T. (1986), Intraseasonal variations of OLR in the Tropics during the FGGE year, *J. Meteorol. Soc. Jpn.*, *64*, 17–34.

Nakazawa, T. (2006), Madden-Julian Oscillation activity and typhoon landfall on Japan in 2004, *SOLA*, *2*, 136–139.

Reynolds, R. W., T. M. Smith, C. Liu, D. B. Chelton, K. S. Casey, and M. G. Schlax (2007), Daily high-resolution blended analyses for sea surface temperature, *J. Clim.*, *20*, 5473–5496, doi:10.1175/2007JCLI1824.1.

Ritchie, E. A., and G. J. Holland (1999), Large-scale patterns associated with tropical cyclogenesis in the western Pacific, *Mon. Weather Rev.*, *127*, 2027–2043, doi:10.1175/1520-0493(1999)127<2027: LSPAWT>2.0.CO;2.

Sobel, A. H., and C. S. Bretherton (1999), Development of synoptic-scale disturbances over the summertime tropical northwest Pacific, *J. Atmos. Sci.*, *56*, 3106–3127, doi:10.1175/1520-0469(1999)056<3106:DOSSDO>2.0. CO;2.

Straub, K. H., and G. N. Kiladis (2003), Interactions between the boreal summer intraseasonal oscillation and higher-frequency tropical wave activity, *Mon. Weather Rev.*, *131*, 945–960, doi:10.1175/1520-0493 (2003)131<0945:IBTBSI>2.0.CO;2.

Takayabu, Y. N. (1994), Large-scale cloud disturbances associated with equatorial waves. Part I: Spectral features of the cloud disturbances, *J. Meteorol. Soc. Jpn.*, *72*, 433–449.

Takayabu, Y. N., and T. Nitta (1993), 3–5 day-period disturbances coupled with convection over the tropical Pacific Ocean, *J. Meteorol. Soc. Jpn.*, *71*, 221–246.

Tam, C.-Y., and T. Li (2006), The origin and dispersion characteristics of the observed tropical summertime synoptic-scale waves over the western Pacific, *Mon. Weather Rev.*, *134*, 1630–1646, doi:10.1175/MWR3147.1.

Wang, B., and J. C. L. Chan (2002), How strong ENSO events affect tropical storm activity over the western North Pacific, *J. Clim.*, *15*, 1643–1658, doi:10.1175/1520-0442(2002)015<1643:HSEEAT>2.0. CO;2.

Wheeler, M., and H. Hendon (2004), An all-season real-time multivariate MJO index: Development of an index for monitoring and prediction,

Mon. Weather Rev., *132*, 1917–1932, doi:10.1175/1520-0493(2004) 132<1917:AARMMI>2.0.CO;2.

Wheeler, M., and G. N. Kiladis (1999), Convectively coupled equatorial waves: Analysis of clouds and temperature in the wavenumber-frequency domain, *J. Atmos. Sci.*, *56*, 374–399, doi:10.1175/1520-0469(1999) 056<0374:CCEWAO>2.0.CO;2.

Wheeler, M., G. N. Kiladis, and P. J. Webster (2000), Large-scale dynamical fields associated with convectively coupled equatorial waves, *J. Atmos. Sci.*, *57*, 613–640, doi:10.1175/1520-0469(2000)057<0613: LSDFAW>2.0.CO;2.

Xie, X., and B. Wang (1996), Low-frequency equatorial waves in vertically sheared zonal flow. Part II: Unstable waves, *J. Atmos. Sci.*, *53*, 3589–3605, doi:10.1175/1520-0469(1996)053<3589:LFEWIV>2.0.CO;2.

Xue, Y., T. M. Smith, and R. W. Reynolds (2003), Interdecadal changes of 30-yr SST normals during 1871–2000, *J. Clim.*, *16*, 1601–1612.

Yanai, M., and T. Maruyama (1966), Stratospheric wave disturbances propagating over the equatorial Pacific, *J. Meteorol. Soc. Jpn.*, *44*, 291–294.

L. Ching, C.-H. Sui, and M.-J. Yang, Department of Atmospheric Sciences, National Taiwan University, Taipei 10617, Taiwan. (sui@as. ntu.edu.tw)